

X-MCD calculations

In this section we discuss the polarization dependence of x-ray absorption spectral shapes. This includes both linear dichroism and circular dichroism.

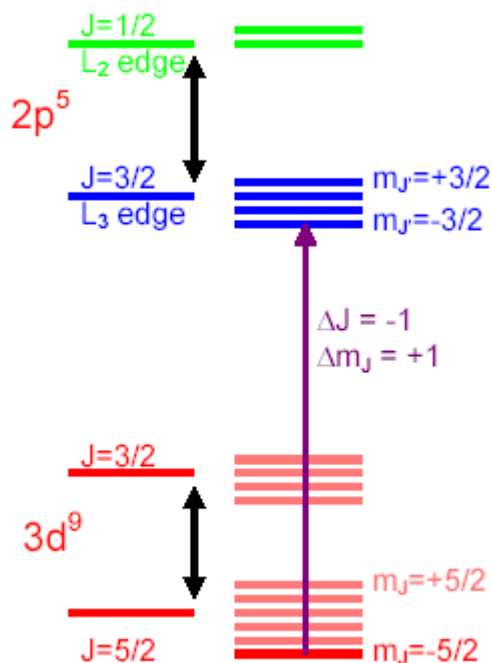
As examples we will use the Cu^{2+} and N^{2+} ground state. Cu^{2+} is given as a $3d^9$ configuration and N^{2+} as a $3d^8$ configuration. We will discuss MCD with atomic multiplets, crystal field effect on X-MCD, charge transfers on X-MCD, the input files for X-MCD calculations and the difference between exchange fields and magnetic fields. At the end we will give a number of examples from 3d-systems, 4d-systems and 4f-systems. Before starting with the examples, X-MCD will be introduced.

Dichroism is the property of certain objects showing different colours according to their orientation with respect to the light. It is due to the dependence of the optical response of the object on the relative orientation between the polarisation direction of the light and the symmetry axes of the object. With x-rays, in some cases a difference can be observed between the absorption of left and right circularly polarised light (Circular Dichroism) or for different orientations of the polarisation vector of linearly polarised light with respect to a given quantization axis (Linear Dichroism). Dichroism can only occur when the spherical symmetry of the free atom is broken due to a magnetic field and/or an electric field such as crystal field effects. Magnetic fields can cause both circular and linear dichroism, while a crystal field can only induce linear dichroism.

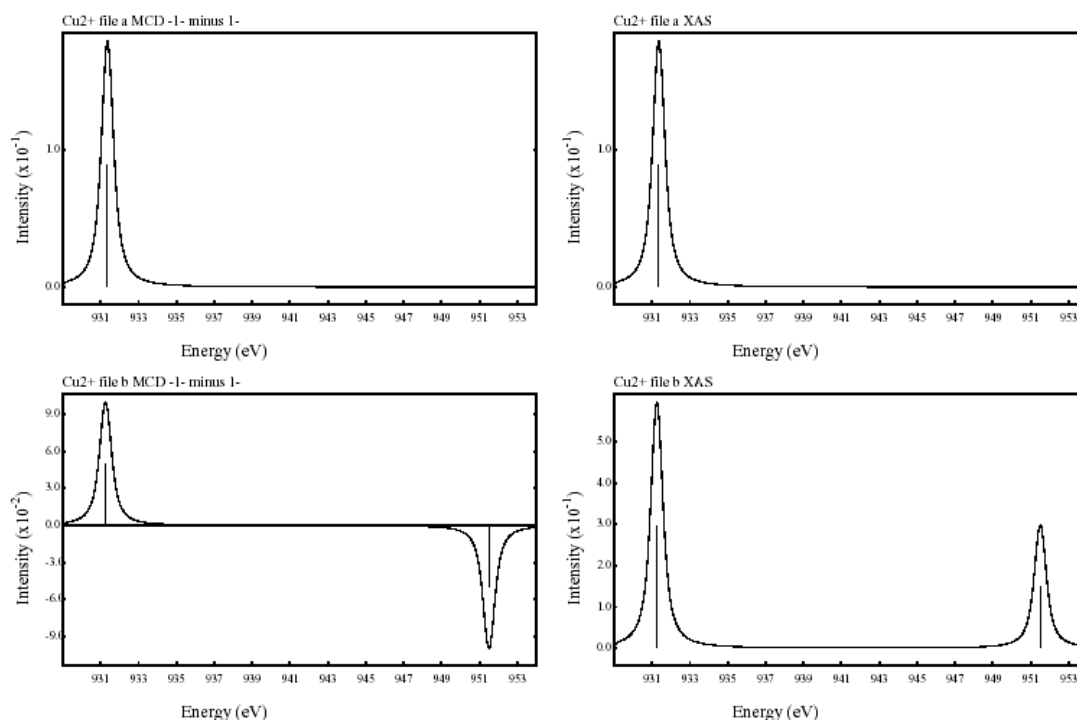
Example of Cu^{2+} .

The initial state of Cu^{2+} has a $2p^63d^9$ configuration, that is it contains a single 3d-hole. This implies that the 3d3d multiple interactions are absent and one only has the crystal field effects, the 3d spin-orbit coupling and the Zeeman exchange field or an external magnetic field. In the final state the 2p core hole spin-orbit coupling is an important factor for the dichroic effects. The final state has a $2p^53d^{10}$ configuration, hence no 3d-holes implying no 2p3d multiplets and no effects of the crystal field, exchange field and 3d spin-orbit coupling.

The initial state has a $3d^9$ configuration, hence the single 3d-hole ground state has $L=2$ and $S=1/2$. Following Hund's rules, its J-value is equal to $L+S = 5/2$. There is an excited state with $J=3/2$. The final state has a single 2p-hole, hence it has a $J=3/2$ state and a $J=1/2$ state, respectively the L3 and the L2 edge. Applying an exchange field splits the J states into their respective M_J sublevels, with the $M_J=-5/2$ as the ground state. The final states have M_J values between $-3/2$ and $+3/2$ and the selection rule states that ΔM_J is equal to -1 , 0 or $+1$ dependent on the polarization of the x-ray. This implies that for this ground state there will be only a single transition. This is the transition from $M_J=-5/2$ to $M_J'=-3/2$, with the $M_J=+1$ operator. The J-value of the ground state is $5/2$ and the J-values of the final states are $J=3/2$ and $J=1/2$. With the dipole selection rules $J = +1, 0$ or -1 , this implies that there is only a transition to the $J=3/2$ final state. That is, the only allowed transition has $J = -1$ and $M_J = -1$. The figure below sketches the situation of the various states. This has been described in detail for the similar case of the $4f^{13}$ ground state of Yb^{2+} systems by Goedkoop in goedkoop88a.



The files [als7cu2a.rcg](#) and [als7cu2a.rac](#) calculate this transition. It is interesting to compare a number of different situations. Let us first assume that the 3d spin-orbit coupling is switched off. The files [als7cu2b.rcg](#) and [als7cu2b.rac](#) calculate this transition and the file [als7cu2ab.plo](#) generates a combined figure for both cases, which is given below.



The top images show the atomic case with the single $J=-5/2$ to $J'=-3/2$ transition. The XAS is given on the right and the identical X-MCD spectrum is given on the left. The X-MCD spectrum is identical because there is only a $\Delta m_J = -1$ transition. The bottom images show the XAS (right) and its MCD (left) for an initial state that is not affected by 3d spin-orbit coupling. Effectively this implies

that the transitions from the $J=3/2$ state are added to those of the $J=5/2$ state. If we look into the als7cu2a.ora output file, we find the following eigen values for the $3d^9$ ground state:

EIGVAL	-0.101095	0.152095	
EIGVAL	-0.103093	0.154093	
EIGVAL	-0.107000	-0.099064	0.150064
EIGVAL	-0.105061	-0.097000	0.156061

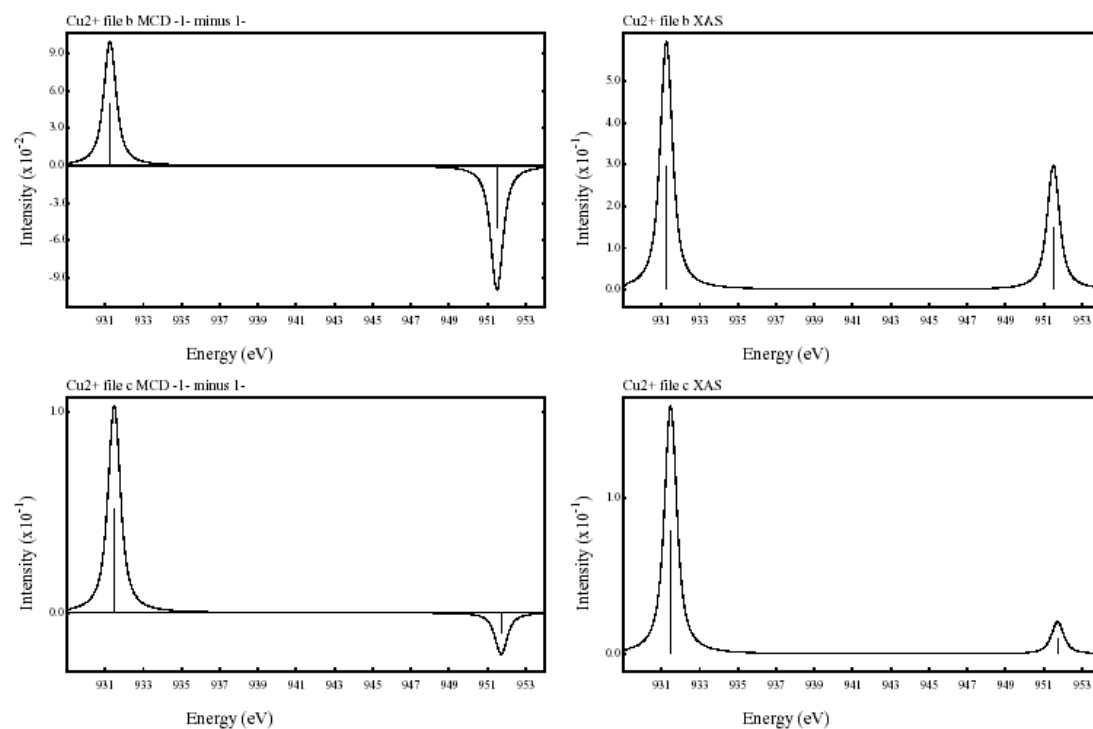
The six $J=5/2$ states are found between -0.107 and -0.097 eV and the four $J=3/2$ states are found between 0.150 and 0.156 eV. The $J=3/2$ state will have transitions to both the L3 edge and the L2 edge. This approximation is exactly the atomic, single electron, model as used by Erskine and Stern [Ers75]. It describes the transitions of the 2p core state to the 3d valence state, where only the 2p spin-orbit coupling is included. This yields the following values:

	++	+-	XAS	MCD
L3	3 ($*R^2/9$)	5	8	+2
L2	3	1	4	-2

The ratio of the XAS of the L3 edge to the L2 edge is 2:1, while their X-MCD ratio is +1:-1 (or -1 to $+1$ depending on the definition used). This single particle ratio is found for all cases where the 3d spin-orbit coupling is zero. It is often assumed that this is the case for the 3d transition metals, which are then analysed with this model. Effectively this also implies the neglect of the multiplet effects.

Next we include a cubic crystal field of 0.304 eV. The files als7cu2a.rcg and als7cu2a.rac calculate this transition. Note that the crystal field strength is given as 1.0; the reason is that the values in the als7cu2a.rac file are NOT in electronvolts. A given value of 1.0 corresponds to a cubic crystal field of 0.304 eV. The result is given in the figure below. If a crystal field of 0.3 eV is added to the ground state, one finds a small L2 edge and also a small X-MCD at the L2 edge. Effectively one finds a result that is in between the situation with and without spin-orbit coupling. The reason for this is that if one includes a cubic crystal field, one effectively mixes the $J=5/2$ and $J=3/2$ states of the 3d-band. In fact, this is the reason that the 3d spin-orbit coupling can/must be neglected in many cases. Due to the crystal field (and other effects, for example translational symmetry), the $J=5/2$ and $J=3/2$ states in the 3d-band are completely mixed.

Exercise: Change the cubic crystal field in the file als7cu2a.rac from 1.0 to 3.28 (relates to 1.0 eV) and then to 10.0. Look what happens to the resulting XAS and X-MCD spectra.



The ground state of Cu^{2+} has been analysed in detail in [saintavit97a.pdf](#). As described above, the interplay between the 2p spin-orbit coupling, 3d spin-orbit coupling, crystal field effects and the exchange splitting determine the ground state and the resulting XAS and X-MCD spectra.

Example of $N2+^I$.

Next we switch to a $N2+^I$ ground state. The difference between $N2+^I$ and Cu^{2+} is that the $3d^8$ ground state is affected by $3d3d$ multiplet effects. In addition, the $2p53d^9$ final state is affected by $2p3d$ multiplet effects. This will completely modify the $2p$ XAS and X-MCD spectra of $N2+^I$ compared with Cu^{2+} . We start with the same calculation as for Cu^{2+} , which is a pure atomic calculation, including all atomic effects (multiplet effects, spin-orbit couplings).

The files `als7ni2a.rcg` and `als7ni2a.rac` calculate the atomic transition for $N2+^I$ and the files `als7ni2b.rcg` and `als7ni2b.rac` calculate the same transition without the inclusion of the $3d$ spin-orbit coupling. The input of the `rcg`-file for X-MCD calculations is analogous to a normal XAS calculation. The only addition is the inclusion of the operator spin and in some cases also orbit. The first line reads:

```
10          14      2      4      1      1  INTER2 shell103000000 %
spin03000000 orbit03000000
```

The % can be used if a line becomes too long. In addition to the crystal field (SHELL), this file adds an exchange field (SPIN) or a magnetic field (SPIN and ORBIT) to the matrices that are calculated.

The `als7ni2a.rac` file is modified a bit more. It reads:

```
Y
  % vertical 1 1
butler O3
to      Oh
to      D4h
to      C4h
endchain
actor   0+ HAMILTONIAN ground  PRINTEIG
OPER HAMILTONIAN
  BRANCH 0+ > 0 0+ > 0+      > 0+      1.0
OPER SHELL2
  BRANCH 4+ > 0 0+ > 0+      > 0+      0.0
  BRANCH 4+ > 0 2+ > 0+      > 0+      0.0
  BRANCH 2+ > 0 2+ > 0+      > 0+      0.0
OPER SPIN2
  BRANCH 1+ > 0 1+ > ^0+    > 0+      0.01
OPER ORBIT2
  BRANCH 1+ > 0 1+ > ^0+    > 0+      0.00
actor   0+ HAMILTONIAN excite  PRINTEIG
OPER HAMILTONIAN
  BRANCH 0+ > 0 0+ > 0+      > 0+      1.0
OPER SHELL2
  BRANCH 4+ > 0 0+ > 0+      > 0+      0.0
  BRANCH 4+ > 0 2+ > 0+      > 0+      0.0
  BRANCH 2+ > 0 2+ > 0+      > 0+      0.0
OPER SPIN2
  BRANCH 1+ > 0 1+ > ^0+    > 0+      0.01
OPER ORBIT2
  BRANCH 1+ > 0 1+ > ^0+    > 0+      0.00
actor   1- left      transi PRINTTRANS
oper MULTIPOLE
  branch 1- > 0 1- > 1- > 1-  1.000
```

```

actor -1- right      transi PRINTTRANS
oper MULTIPOLE
  branch 1- > 0 1- > 1- > -1- 1.000
actor 0- parallel    transi PRINTTRANS
oper MULTIPOLE
  branch 1- > 0 1- > ^0- > 0- 1.000
RUN

```

Important is that the symmetry is changed from O3, via Oh and D4h to C4H. This allows one to add an exchange field with the operator SPIN2. The exchange field is added in electronvolts and has a value of 0.01, or 10 meV. Note that the dipole operator splits into left (1-), right (-1-) and parallel (0-) due to the symmetry lowering from O3 to C4H. C4H symmetry implies that the magnetic field is added in the z-direction of the tetragonal symmetry. This inputfile allows one to add crystal field parameters (X40, X42 and X22) and an exchange or magnetic field.

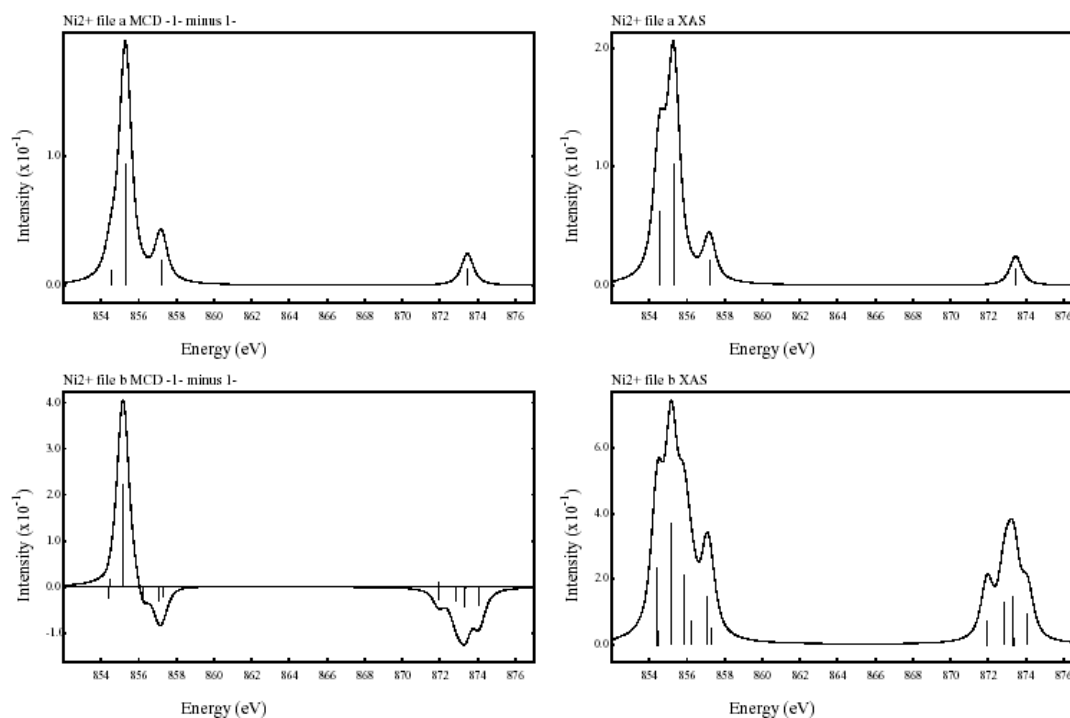
The file als7ni2ab.plo generates a combined figure for both cases, which is given below. The new commands/lines for X-MCD calculations are:

```

frame_title N2+1 file b MCD -1- minus 1-
addlines operator -1-
spectrum operator 1- scale -1

```

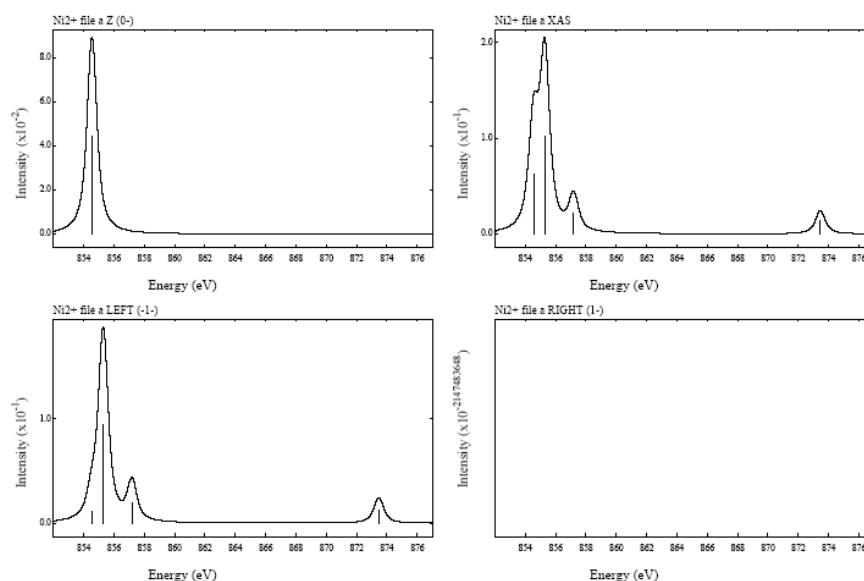
These three lines give the X-MCD spectrum in a separate figure. **frame_title** gives the title of the frame. **Addlines** makes a spectrum for the operator -1-, but instead of plotting it, it saves the spectrum in memory. The command **spectrum** creates the spectrum for operator 1- multiplied with the scale factor of -1. In addition it adds all stored spectra. Together these two lines create a spectrum of the operator -1- minus the operator 1-. Alternatively, one can just calculate the spectra of the three individual operators (-1-, 0- and 1-) and use their spectra in separate software to create the figures.



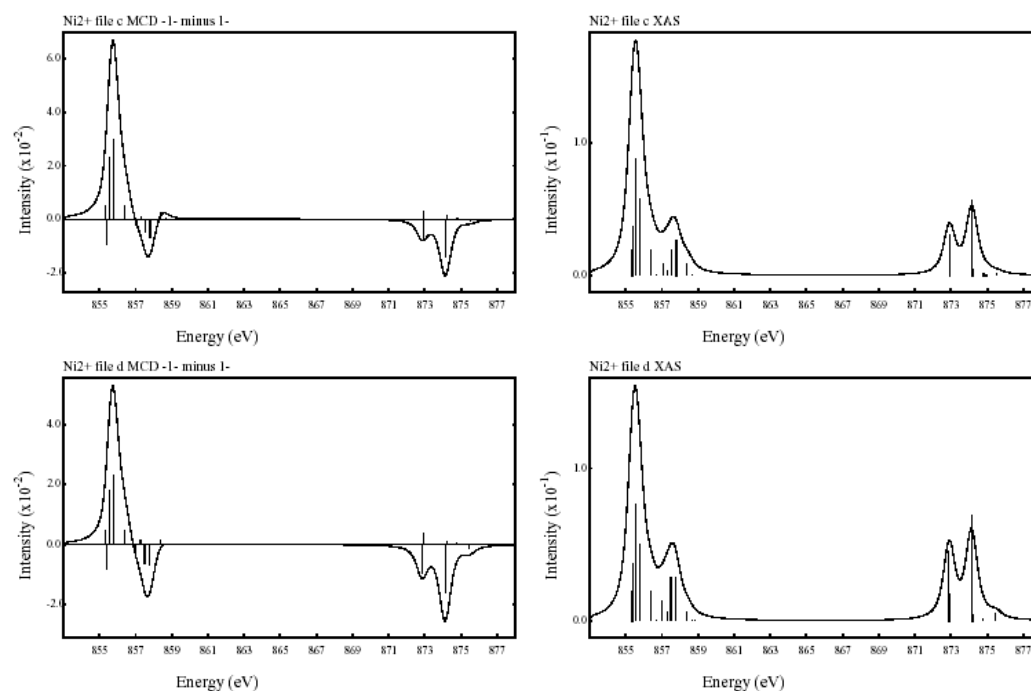
The XAS figures on the right are the same as given in chapter3 for als3ni2c and als3ni2d. The MCD figures on the right show that the MCD effect for atomic $N2^{+1}$ including the 3d spin-orbit coupling is completely positive. The reason is that there are no allowed transitions for right polarized x-rays. This is closely related to the figure in chapter 3 that separated the J' values of the final state. The first peak relates to a transition from the ground state $3F4$ state to a $J=4$ final state. The other three peaks relate to a $J=3$ final state. The $J=-1$ transitions are purely left polarized ($m_j=-1$), as can be checked from table 17, reproduced from degroot94a.pdf. The transition from $J=4$ to $J'=4$ can have either $m_j=-1$ or $m_j=0$ transitions, but no $m_j=+1$ transitions. Together this implies that the whole MCD spectrum (left-right) is positive. A more general table is given below.

Table 17
Correlation between ΔJ and ΔM_J

ΔJ	$(\Delta M_J = -q)$		
	-1	0	+1
-1	1	0	0
0	$\frac{1}{J+1}$	$\frac{J}{J+1}$	0
+1	$\frac{1}{(2J+3)(J+1)}$	$\frac{2J+1}{(2J+3)(J+1)}$	$\frac{(2J+1)(J+1)}{(2J+3)(J+1)}$



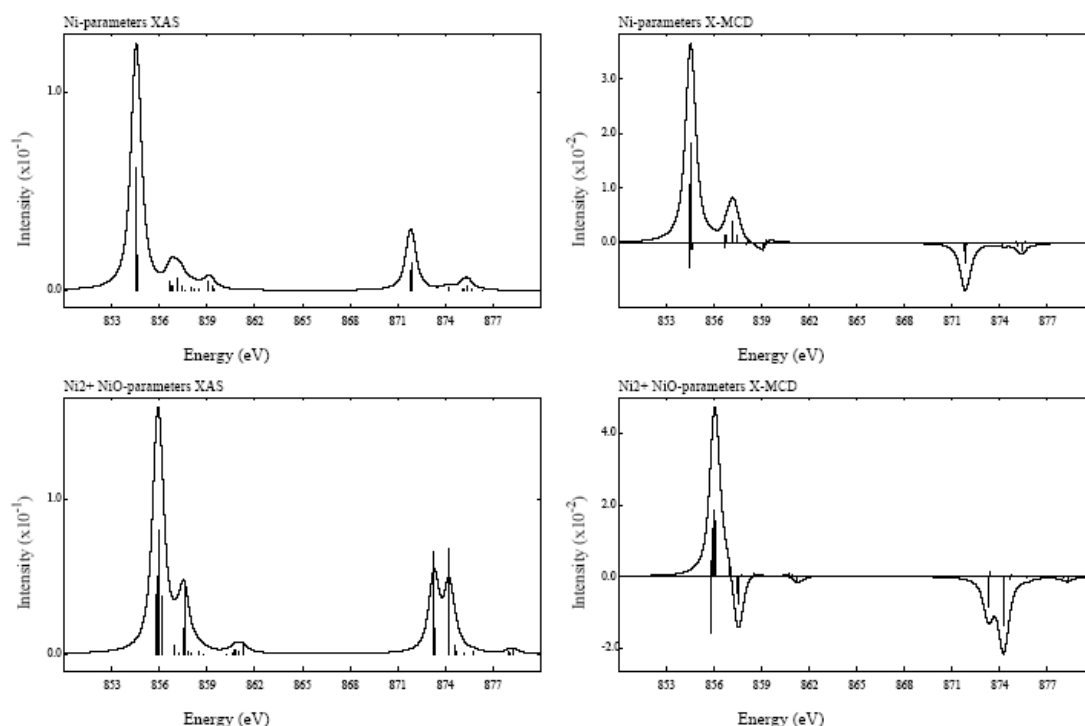
Applying a cubic crystal field modifies the ground state to $3A_2$. We have seen in chapter 5 that the 3d spin-orbit coupling has only a minor effect in case of a $3A_2$ ground state. This is confirmed in the X-MCD spectra of $N2^{+1}$ in octahedral symmetry. The files als7ni2c.rcg and als7ni2c.rac calculate the crystal field transition for $N2^{+1}$ and the files als7ni2d.rcg and als7ni2d.rac calculate the same transition without the inclusion of the 3d spin-orbit coupling. The file als7ni2cd.plt generates a combined figure for both cases, which is given below.



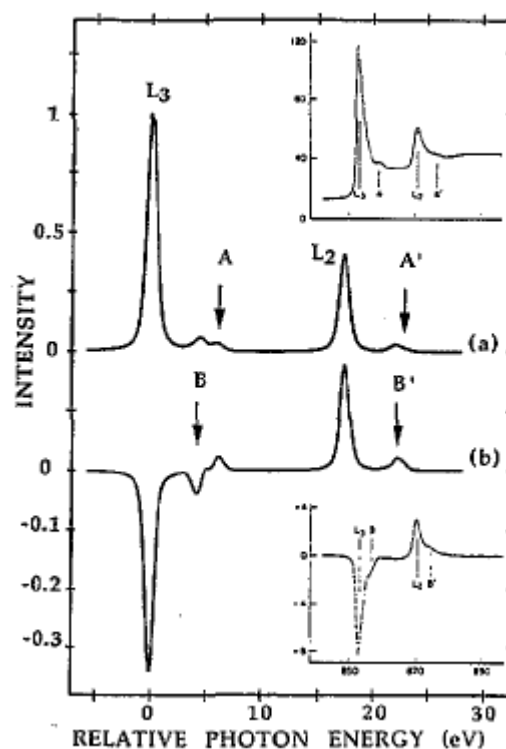
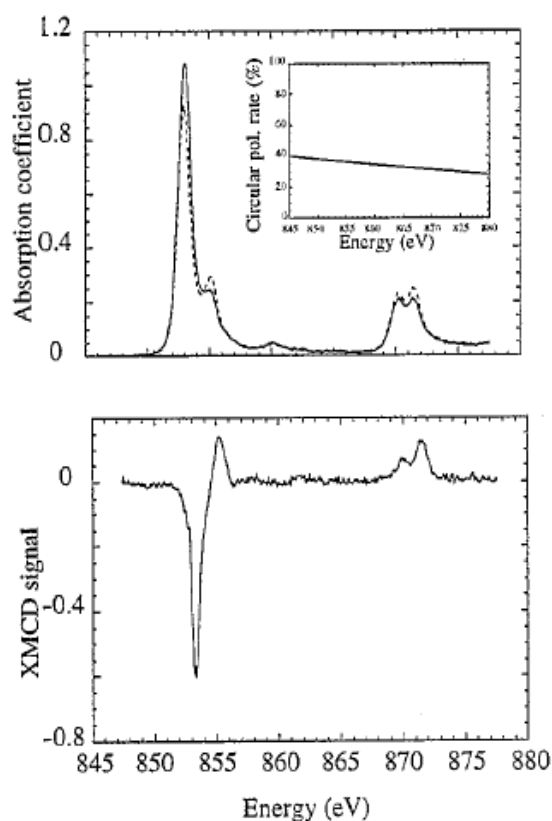
The figures show the similar 2p XAS and X-MCD spectra of Ni^{2+} in an octahedral crystal field with (top) and without (bottom) the inclusion of 3d spin-orbit coupling. It is interesting to note that though the ground state has 3A_2 character, there is still a visible effect of the 3d spin-orbit coupling. The reason is the admixture of states of other character. This implies that the ground state is not 100% 3A_2 symmetry if 3d spin-orbit coupling is included. (It is 100% a T_2 symmetry state in the double group description, but the 3A_2 -type T_2 state has a little admixture of T_2 states of other (high-energy) T_2 states. In total there are 6 T_2 states as we have seen when generating the TSD in chapter 5.

Charge transfer and the X-MCD spectral shape for $N2+^I$ ions and Ni metal

The next step is to include charge transfer for X-MCD calculations. The procedure is analogous to the XAS calculations. The files als7ni2ctc4.rcg, als7ni2ctc4.rac and als7ni2ctc4.ban calculate the charge transfer multiplet spectrum, including its X-MCD. The files als7ni2ctc4.rcg and als7ni2ctc4.rac contain no new features. Compared with charge transfer XAS calculations as explained in chapter 6, the rcg-file adds the matrices of the spin-operator. The rac-file branches to C4H symmetry, similar to the case without charge transfer. Also the ban-file is similar. It contains the TRIADS related to C4H symmetry, that is with the three different operators and it contains an additional term in the Hamiltonian that gives the SPIN (= exchange) field.



This figure gives at the bottom the XAS and X-MCD spectra for a $N2+I$ ion (using the parameters of NiO). The top spectra are the XAS and X-MCD spectra using the parameters for Ni metal.



These figures contain the experimental spectra of a Ni^{2+}I cyanide complex (left, from arrio96a.pdf) and Ni metal compared with CTM calculations (right, from vanderlaan92a.pdf). These experimental spectra are similar to the CTM calculations as given above.

There is a special feature for the calculation of Ni metal. The CTM parameters for Ni metal have been determined from XPS spectra. As will be explained in chapter 8, XPS needs more than two configurations in the ground state to arrive at a decent description of the spectral shapes. This implies that Ni metal is approximated as a linear combination of $3d^8$, $3d^9$ and $3d^{10}$. The $3d^{10}$ configuration is not important for 2p XAS because it cannot accept another 3d-electron. However in order to use a consistent model, the $3d^{10}$ configuration is added to the ground state. This yields a CTM calculation with 3 initial and two final state configurations.

General background of X-MCD

The matrix element for a dipole transition from an initial state with quantum numbers J and M to a final state with J' and M' is given by $|\langle J' M' | P_q | J M \rangle|^2 =$

$\left(\begin{matrix} J & 1 & J' \\ -M & q & M' \end{matrix} \right)^2 |\langle J || P_q || J' \rangle|^2$. Here, the matrix element is split into an angular (the 3-j symbol)² and a radial part using the Wigner-Eckart theorem.

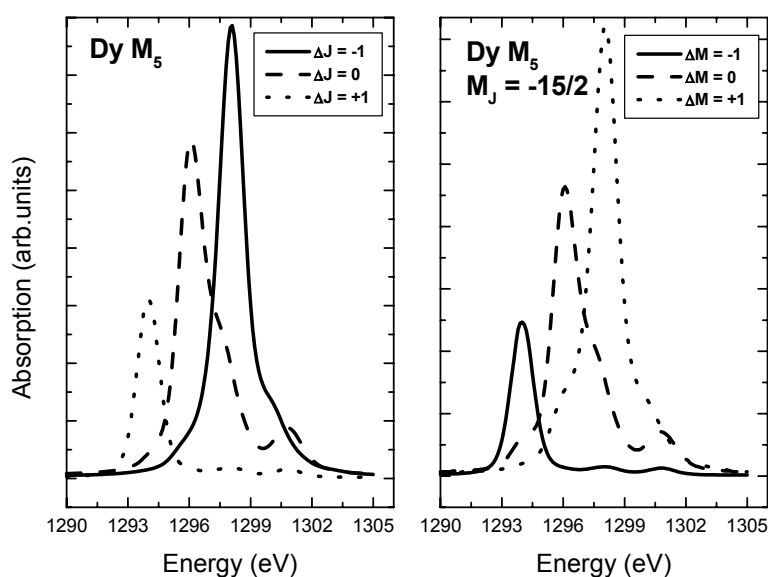
The radial part $|\langle J || P_q || J' \rangle|^2$ is also called the line strength of the transition. The dependence of the absorption on the polarisation of the light is caused by the dependence of the 3J-symbols on M . The 3J-symbol is non-zero only if $|J - J'| \leq 1$, $J + J' + 1$ and $q = M' - M = 0, \pm 1$. Transitions with $q=0$ can be excited only by radiation that has a linearly polarised component along the z-axis (i.e. the quantization axis) and $q = \pm 1$ transitions only by components that are left- respectively right-handed circularly polarised in the plane perpendicular to this axis. The relation between the J transitions and the polarisation is given in Table 5.1.

$J \backslash q$	-1	0	1
-1	$\frac{J(J-1) - (2J-1)M + M^2}{2J(2J+1)(2J-1)}$	$\frac{J^2 - M^2}{J(2J+1)(2J-1)}$	$\frac{J(J-1) + (2J-1)M + M^2}{2J(2J+1)(2J-1)}$
0	$\frac{J(J+1) - M - M^2}{2J(2J+1)(2J-1)}$	$\frac{M^2}{J(2J+1)(J+1)}$	$\frac{J(J+1) + M - M^2}{2J(2J+1)(J+1)}$
1	$\frac{(J+1)(J+2) + (2J+3)M + M^2}{2(2J+3)(2J+1)(2J-1)}$	$\frac{(J+1)^2 - M^2}{(2J+3)(2J+1)(J+1)}$	$\frac{(J+1)(J+2) - (2J+3)M + M^2}{2(2J+3)(2J+1)(2J-1)}$

Table 5.1 The relation between J transitions and the polarisation vector q .

In spherical symmetry, the Hund's rule ground state is $(2J+1)$ -fold degenerate and all M_J -levels are equally populated. It can be shown that in that case the polarisation of the light does not have any influence on the absorption spectrum (Sacchi and Vogel 2001). A magnetic or crystalline electric field splits up the ground state in levels with different values of M_J and at low enough temperature levels with different M_J will be unequally occupied. The simplest example is for an Yb^{2+} ion in an applied magnetic field. The magnetic field will cause a Zeeman splitting of the levels of the $^2F_{7/2}$ ground state in fifteen levels with $M_J = -7/2, -5/2, \dots, 7/2$ and energy $\mu_B g M_J$. At zero Kelvin, only the lowest lying level, with $M_J = -7/2$, will be occupied. In the final state, only the $^2D_{5/2}$ state is available, with $-5/2 \leq M_J \leq 5/2$.

As a result, at zero Kelvin only $M = +1$ transitions can take place, so only left circularly polarised light or linearly polarised light, incident along the quantization (in this case, the magnetisation direction) axis. Right circularly polarised light, or linearly polarised light with its polarisation vector parallel to the magnetisation axis will not be absorbed. At higher temperatures, also higher M_J -levels will be occupied, according to a Boltzman distribution, and the other transitions (first $M = 0$ for $M_J = -5/2$, than also $M = -1$ for $M_J = -3/2$) will become possible. However, some polarisation dependence of the absorption spectra will persist until $kT \gg \mu_0 g_J H$. X-ray Dichroism can thus be used to measure magnetic ordering, with the element selectivity inherent to X-ray Absorption Spectroscopy. It can be shown that circular dichroism (difference between $M = +1$ and $M = -1$ transitions) is proportional to $\langle M_J \rangle$, the average M_J - value of the ion, which corresponds to its magnetic moment ($|M| = \langle M \rangle \mu_0 g_J$). Linear dichroism is related to $\langle M_J^2 \rangle$, the average of the square of M_J . It is therefore sensitive to magnetic order, but it can not give the sign, or direction, of the magnetic moments. In contrast to (magnetic) circular dichroism, linear dichroism is also sensitive to crystalline electric fields with a less than cubic symmetry. This often limits the interest of linear dichroism for magnetic studies of rare earths, since in



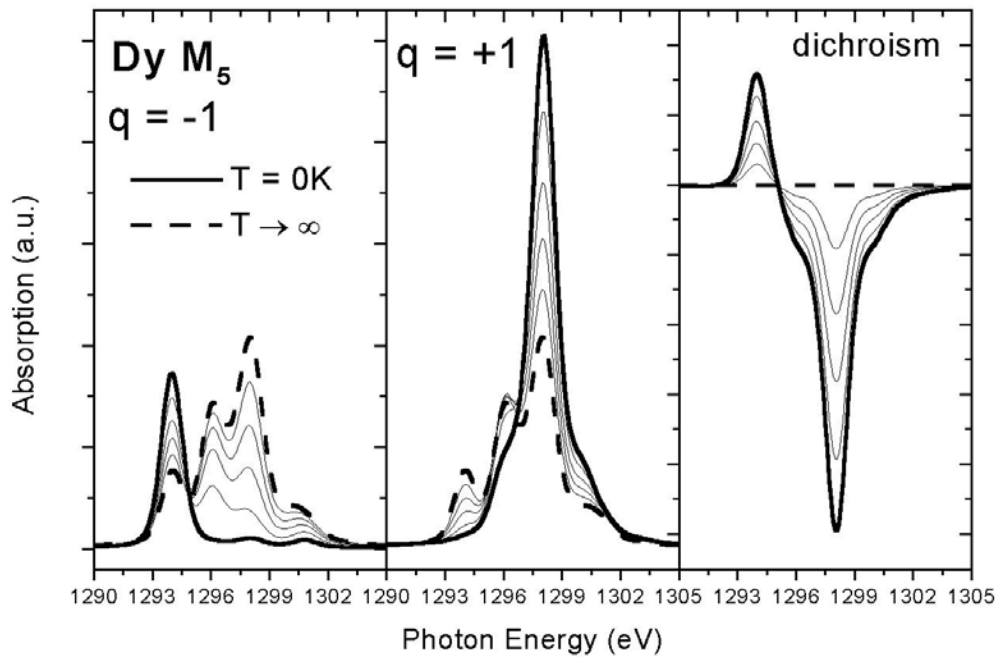
many magnetic compounds containing rare earths the rare earth ion is in a low symmetry crystal field environment.

Figure 5.1 (left) The calculated J components for the M_5 -edge of Dy (ground state $^6H_{15/2}$). (right) The different M -transitions for the lowest lying level in a magnetic field, $M_J = -15/2$.

As discussed in chapter 2, in many rare earth $M_{4,5}$ -edges three peaks are visible corresponding to the different J -transitions. The cross-section σ_J^q for a transition from a single ground-state level $|JM_J^k\rangle$ of the free ion to all final states allowed by the selection rules and for a photon polarisation q is given by $\sigma_J^q = \sum_{J'} |3J\text{-symbol}|^2_{JJ'}$. This means that for any M_J -level and any $q = M$, the transition can be written as a linear combination of the three J components. As an example, in Figure 5.1. we give the calculated J components for the M_5 -edge of Dy (ground state $^6H_{15/2}$). In the same figure, we give the different M -transitions for the

lowest lying level in a magnetic field, $M_J = -15/2$. As can be seen, the M -transitions closely correspond to J -transitions. For the other M_J -levels, every M contains the three J -components, with different weights. The occupation of the different M_J -levels, which depends on the splitting as well as the temperature, determines therefore the polarisation dependence of the spectrum.

As an example, we give in Fig. 5.2 the spectra for left- and right circularly polarised light, as well as their difference (the circular dichroism) as a function of temperature for a Dy^{2+} ion in a magnetic field. The spectra and dichroism are given for different values of the reduced temperature $T_R = kT / \mu_B g H$, where μ_B is the Bohr magneton, g is the Landé factor and H is the magnetic field strength. $\mu_B g H$ defines the splitting between the different Zeeman levels and kT their occupation. This shows that in general the spectra depend both on the (internal) magnetic field acting on the ion and on the temperature. The size of the dichroism gives a direct measure of the average magnetic moment in the direction of propagation of the X-rays. The right panel of Fig. 5.2 shows that the size of the dichroism depends on the temperature and magnetic field, but that the shape of the curves does not change. It can be shown that this is generally the case for both circular and linear dichroism in Rare Earths (see for instance J.Ph.Schillé and others, PRB 48, 9491 (1993)), as long as the energy between the



Hund's rule ground state and the first excited state is large.

Figure 5.2: Calculated M_5 -edge absorption for a Dy^{2+} -ion in a magnetic field for right (first panel) and left (second panel) circularly polarised light. The difference (or XMCD) curves are given on the right. The spectra are for different values of the reduced temperature T_R (see text), with $T_R = 0, 2, 4, 7, 15$ and T_R

In a crystal field, the M_J -levels are split according to their absolute value $|M_J|$, i.e. every energy level is a mixture of different M_J -levels, where M_J and $-M_J$ have the same weight. Since the spectra for M_J , M are the same as for $-M_J$, $-M$ a crystal field can not introduce circular dichroism. However, a crystal field with a symmetry lower than cubic will give rise to linear dichroism, like ferromagnetic but also antiferromagnetic ordering.

For metallic Transition Metal-atoms, the d-electrons are delocalised (or itinerant) and the atomic approach for the absorption and dichroism is not valid. This can be partly overcome using a configuration interaction approach, where the ground state of the absorbing atom is written as the superposition of atomic states of different d-count, with different weights. In most cases, band-structure effects play an important role in the shape of spectra of metallic transition metals, and a one-electron approach is generally used to treat the excitations.

More soon:

1. X-MCD and LD for rare earths
2. Sum rules
3. Theoretical tests of the sum rules (calculation of moments, large 2p spin-orbit coupling)
4. Different directions for the magnetic field

Testing the sum rules with the multiplet calculations

More soon.